doi:10.1016/j.jmb.2008.05.071 J. Mol. Biol. (2008) 380, 958–971

JMB

Available online at www.sciencedirect.com

ScienceDirect

ELSEVIER

Structure of the BH3 Domains from the p53-Inducible BH3-Only Proteins Noxa and Puma in Complex with Mcl-1

Catherine L. Day[1], Callum Smits[1], F. Cindy Fan[2], Erinna F. Lee[2], W. Douglas Fairlie[2] and Mark G. Hinds[2]*

[1]*Department of Biochemistry, University of Otago, Dunedin 9054, New Zealand*

[2]*Walter and Eliza Hall Institute of Medical Research, 1G Royal Parade, Parkville 3050, Australia*

Received 18 March 2008; received in revised form 29 May 2008; accepted 29 May 2008
Available online 4 June 2008

Pro-survival proteins in the B-cell lymphoma-2 (Bcl-2) family have a defined specificity profile for their cell death-inducing BH3-only antagonists. Solution structures of myeloid cell leukaemia-1 (Mcl-1) in complex with the BH3 domains from Noxa and Puma, two proteins regulated by the tumour suppressor p53, show that they bind as amphipathic α-helices in the same hydrophobic groove of Mcl-1, using conserved residues for binding. Thermodynamic parameters for the interaction of Noxa, Puma and the related BH3 domains of Bmf, Bim, Bid and Bak with Mcl-1 were determined by calorimetry. These unstructured BH3 domains bind Mcl-1 with affinities that span 3 orders of magnitude, and binding is an enthalpically driven and entropy–enthalpy-compensated process. Alanine scanning analysis of Noxa demonstrated that only a subset of residues is required for interaction with Mcl-1, and these residues are localised to a short highly conserved sequence motif that defines the BH3 domain. Chemical shift mapping of Mcl-1:BH3 complexes showed that Mcl-1 engages all BH3 ligands in a similar way and that, in addition to changes in the immediate vicinity of the binding site, small molecule-wide structural adjustments accommodate ligand binding. Our studies show that unstructured peptides, such as the BH3 domains, behave like their structured counterparts and can bind tightly and selectively in an enthalpically driven process.

Keywords: Bcl-2; BH3-only; Mcl-1; enthalpy–entropy compensation; intrinsically unstructured protein

Edited by M. F. Summers

Introduction

In mammals, a group of approximately 20 proteins in the B-cell lymphoma-2 (Bcl-2) family regulates mitochondria-initiated apoptosis, or programmed cell death, a process critical in development, homeostasis and disease for removing unwanted, damaged or diseased cells. At a molecular level, the mechanism of action of Bcl-2 proteins is still poorly defined, but they control the integrity of the mitochondrial outer membrane and modulate release of factors, such as cytochrome *c*, that induce a proteolytic cascade that destroys the cell.[1] Members of the Bcl-2 family are classified as either pro-survival or pro-apoptotic, and the balance between these opposing factions determines whether a cell lives or dies.[2] Interactions between the pro- and anti-survival Bcl-2 proteins are central to apoptosis regulation, and these protein–protein interactions are mediated by regions of conserved sequence known as Bcl-2 homology (BH) domains, of which there are four, BH1 to BH4. Multiple BH domain-bearing Bcl-2 proteins include the pro-survival proteins Bcl-2, Bcl-x_L, Bcl-w, myeloid cell leukaemia-1 (Mcl-1) and A1 and the structurally homologous pro-apoptotic proteins Bax and Bak, each having two to four BH motifs. In contrast, the pro-apoptotic 'BH3-only' proteins, which include Bim, Bad, Bmf, Bid, Bik, Hrk, Puma

*Corresponding author. E-mail address: mhinds@wehi.edu.au.

Abbreviations used: Bcl-2, B-cell lymphoma-2; BH, Bcl-2 homology; HSQC, heteronuclear single quantum coherence; ITC, isothermal titration calorimetry; IUP, intrinsically unstructured protein; Mcl-1, myeloid cell leukaemia-1; NOE, nuclear Overhauser enhancement; NOESY, nuclear Overhauser enhancement spectroscopy; PBS, phosphate buffered saline; SPR, surface plasmon resonance.

and Noxa, bear only BH3 domains.[3] Interactions between BH3-only proteins and their pro-survival counterparts are pivotal to apoptosis regulation.[4,5]

The BH3-only proteins act as cellular sentinels and after an apoptotic stimulus are activated to bind and neutralise the pro-survival Bcl-2 proteins, allowing Bax and Bak to compromise the integrity of mitochondria.[6] Structural studies have shown that the BH3 domain of BH3-only proteins binds as an amphipathic helix in a surface-exposed hydrophobic groove of the pro-survival protein.[7] The core of the BH3 domain is formed by the sequence motif LXXXGDE (X is any residue),[8] and the conserved leucine and aspartic acid form key interactions with the cognate pro-survival protein. The leucine is buried in the protein–protein interface and packs against conserved residues provided by the pro-survival protein, while the solvent-exposed aspartate forms an ionic interaction with a conserved arginine in the BH1 domain of the pro-survival protein.[5] Other binding interactions arise from three other hydrophobic residues that project into pockets provided that they are part of the exposed hydrophobic groove on the pro-survival protein. All pro-survival proteins use the equivalent interface to bind multiple BH3 ligands,[7,9,10] but they have distinct BH3 binding profiles.[11]

Mcl-1 is a pro-survival Bcl-2 protein that plays a critical role in development and tissue homeostasis, is expressed in a range of tissues in the adult and blocks apoptosis induced by a variety of stimuli.[12] Gene knockout studies showed that Mcl-1 is required for embryonic and immune cell development,[13,14] while its overexpression is implicated in cancer and resistance to treatment.[12] Earlier structural studies showed that the C-terminal region of Mcl-1 has a topology similar to that of other multi-domain Bcl-2 family members and binds BH3-only proteins in its surface-exposed hydrophobic groove, while the N-terminal region (~150 residues) was predicted to be unstructured; in addition, when the latter region is deleted, Mcl-1 retained binding to BH3-only proteins.[15] *In vitro* binding studies established the BH3-only binding profile for Mcl-1, showing that it binds tightly to the BH3 domains of Bim, Bid, Puma and Noxa but not to those of other BH3-only proteins.[11] However, the structural basis of this BH3-only selectivity is not well understood.

A detailed analysis of the interactions of Mcl-1 with its BH3-only protein partners not only is of interest to understand the molecular basis of apoptotic signalling through Mcl-1 but also may lead to the development of new cancer therapies aimed at directly activating apoptosis in tumour cells.[16] Here we investigated the binding interactions of peptides spanning the BH3 domains of pro-apoptotic proteins with Mcl-1 using a combination of structural, thermodynamic and biochemical approaches. The BH3 domain proteins are intrinsically unstructured in the absence partners,[17] but solution structures show that they couple folding with binding of the hydrophobic groove of Mcl-1. Mapping the BH3-only binding site on Mcl-1 using ^{1}H,^{15}N heteronuclear single quantum coherence (HSQC) spectra and amide chemical shift data shows that Mcl-1 undergoes a similar conformational change on binding any of its ligands. We also demonstrate that the association of the BH3 domains with Mcl-1 is dominated by the enthalpic contribution and that the process is enthalpy–entropy compensated, which are both features typical of other protein–protein interactions[18] but not widely appreciated for interactions of intrinsically unstructured proteins (IUPs). Consistent with entropy–enthalpy compensation for these interactions, our chemical shift mapping experiments indicate a redistribution of internal non-covalent interactions within Mcl-1 upon ligand binding. Using alanine scanning, we demonstrated the ability of Mcl-1 to accommodate mutations in the BH3 domain of Noxa but retain its high-affinity binding, a finding compatible with the role of Mcl-1 in binding IUPs, such as Puma, Noxa and Bim, and the intrinsic conformational flexibility of Mcl-1 and its partners.

Results

Solution structures of Noxa and Puma BH3 domains bound to Mcl-1

We determined the solution structures of the C-terminal Bcl-2 domain of mouse Mcl-1 bound to the BH3 domains of mouse Puma and NoxaA, the N-

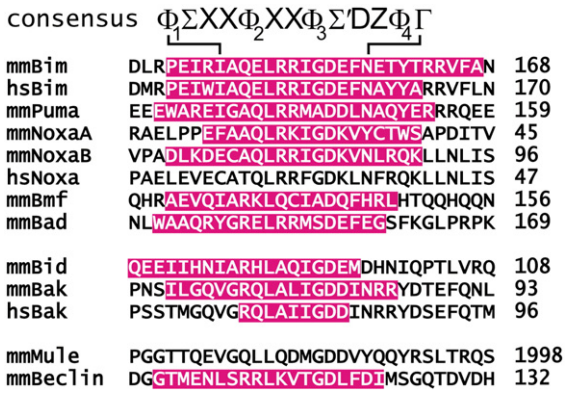

Fig. 1. Sequences and structures of BH3 domains: Sequence alignment of BH3 domains showing the extent of the helices (pink bars) of the BH3 domains when in the bound form [mmBcl-x_L:mmBim, Protein Data Bank (PDB) code 1PQ1[9]; mhMcl-1:hsBim, PDB code 2NL9[10]; mmMcl-1:mmPuma, PDB code 2ROD; mmMcl-1:mmNoxaA, PDB code 2ROC; mmMcl-1:mmNoxaB, PDB code 2JM6[10]; mmA1:mmBmf, PDB code 2VOG[19]; mmBcl-x_L:mmBad, PDB code 2BZW; mmA1:mmBad, PDB code 2VOI[19]; hsBcl-x_L:hsBak, PDB code 1BXL[7]; mmA1:mmBak, PDB code 2VOH[19]; mmBcl-x_L:mmBeclin, PDB code 1P1L[20]]. Key consensus residues that define the BH3 domain are indicated; Φ_1–Φ_4 are hydrophobic residues, Σ and Σ' are small residues, Z is usually an acidic residue, Γ is a hydrophilic residue capable of forming an intermolecular helix cap and X is any residue. Φ_2 is the conserved leucine, and D the conserved aspartate. The sequence position of the C-terminal residue is indicated on the right. hs, *Homo sapiens*; mm, *Mus musculus*; mh, mouse–human chimera.[10]

terminal BH3 domain of dual-BH3 domain-bearing mouse Noxa that differs in sequence from its C-terminal counterpart, NoxaB (Fig. 1). The Bcl-2 domain of Mcl-1 and BH3 domain peptides were prepared as outlined previously.[10,15,17] For each Mcl-1 complex, two samples consisting of ^{13}C,^{15}N-labelled peptide in the presence of unlabelled Mcl-1 and the complementary sample of unlabelled peptide with labelled Mcl-1 were prepared. These samples, combined with X-filtering and editing methods, allowed intermolecular and intramolecular nuclear Overhauser enhancements (NOEs) to be separated.[21] Essentially complete resonance assignments were achieved for both Mcl-1 complexes using a standard array of multi-dimensional NMR techniques.[21] Structures were calculated using CYANA and refined with Xplor-NIH as previously described[15] (Fig. 2). The structures are energetically reasonable, display acceptable covalent geometry and do not have any distance violation >0.2 Å or any angle violation >5° (Table 1). Mcl-1 has a similar structure in both cases and is composed of eight α-helices in which the central hydrophobic helix, α5, is enveloped by the other seven helices (Fig. 2).[15] The secondary structure for each complex was determined by consensus over the final 20 structures using PROCHECK_NMR.[22] The consensus secondary structure for the Mcl-1:NoxaA complex is composed of helices on Mcl-1 α1 (residues 153–172), α2 (185–204), α3 (206–214), α4 (222–234), α5 (242–261), α6 (265–281), α7 (284–289) and α8 (293–300) as well as the NoxaA BH3 helix (residues 22–39). The secondary structure of the Mcl-1:Puma BH3 complex followed that for Mcl-1:NoxaA except for the extent of helix α1 (residues 154–172), helix α3 (residues 206–215) and the Puma BH3 helix (residues 132–153). In both Mcl-1 complexes, the BH3 domain peptides of NoxaA and Puma form amphipathic helices, with their hydrophobic faces lying in a shallow groove formed from residues located on helices α2–α5 and α8 in Mcl-1 (Fig. 2).

When bound to a BH3 domain, Mcl-1 has a conformation that is close to that observed in the absence of ligand. The rmsd between the free and bound forms of Mcl-1 is 1.42±0.13 Å when compared over the secondary structural elements α2–α8 of free Mcl-1.[15] The main conformational change on binding involves translation of the C-terminus of α4 away from the α2–α3 kink, such that the width of the groove accommodating the BH3 domain helix is

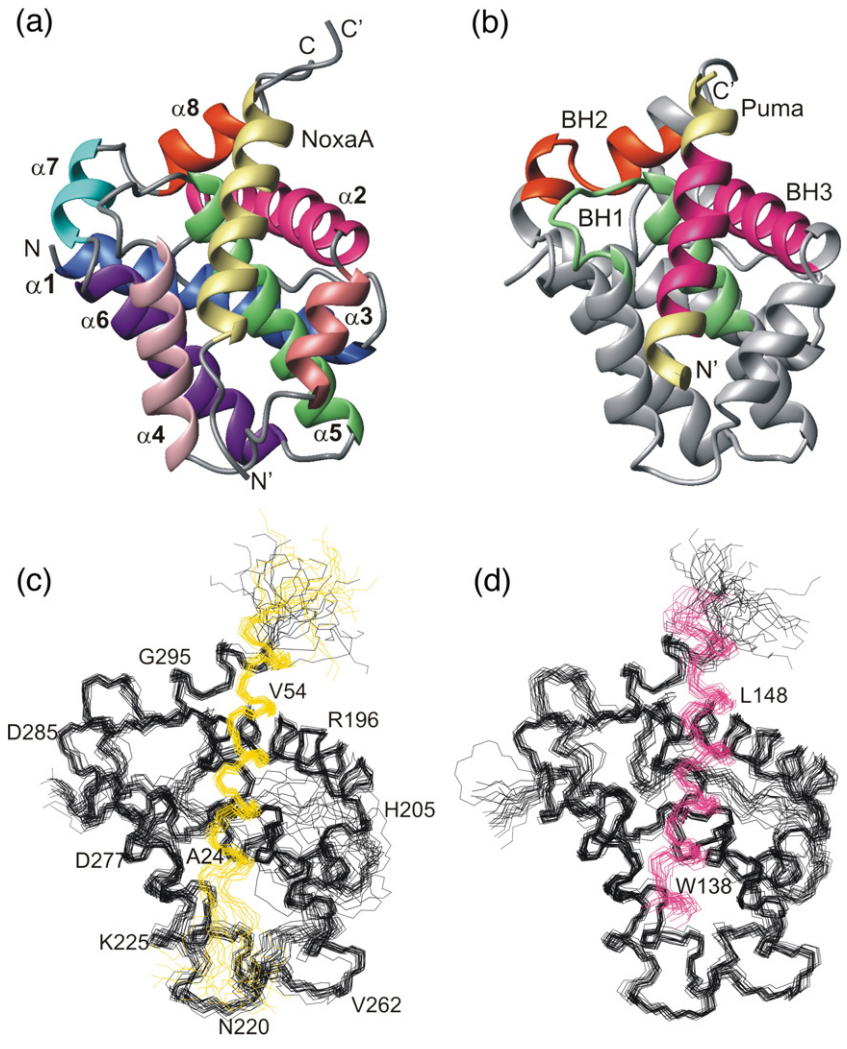

Fig. 2. Ribbon and backbone diagrams of Mcl-1 complexes of NoxaA and Puma BH3 domains. (a) Mcl-1:NoxaA BH3 complex (PDB code 2ROD). The helices are labelled α1–α8, and the N- and C-termini of Mcl-1 are labelled as N and C for Mcl-1 and as N′ and C′ for NoxaA. (b) Mcl-1:Puma BH3 ribbon (PDB code 2ROC). The BH domains of Mcl-1 are coloured as follows: BH1, green; BH2, orange; BH3, pink; Puma BH3, pink. (c and d) Backbones of the 20 NMR-derived structures of Mcl-1 complexes (c) NoxaA BH3 and (d) Puma BH3. For the ribbons in (a) and (b), the structure closest to average was chosen and the secondary structure depicted is the consensus. Residues 152–304 of Mcl-1, residues 17–43 of NoxaA and residues 132–154 of Puma are shown, and sequence numbers are indicated. The same orientation is shown in each case, and the secondary structure depicted by ribbons is that listed in Results.

Table 1. Summary of restraints and structural statistics for the 20 lowest energy structures of Mcl-1ΔNC23:NoxaABH3 and Mcl-1ΔNC23:PumaBH3 at pH 6.7 and 25 °C

	Mcl-1:NoxaA (2ROD)		Mcl-1:Puma (2ROC)	
Experimental constraints				
Total	3355		3667	
Intraresidue	849		788	
Sequential ($\|i-j\|=1$)	543		611	
Short range ($1<\|i-j\|<5$)	545		591	
Long range ($\|i-j\|\geq 5$)	542		756	
Intermolecular	183		197	
Hydrogen bonds	184		188	
Dihedral angles (ϕ, 175; ψ, 150) (ϕ, 174; ψ, 174)	325		348	
rmsd from experimental distance restraints (Å)	0.0102±0.0009		0.01003±0.0009	
rmsd from experimental dihedral restraints (°)	0.38±0.06		0.44±0.06	
rmsd from idealised covalent geometry				
Bonds (Å)	0.00478±0.00005		0.00496±0.00003	
Angles (°)	0.43±0.01		0.43±0.01	
Impropers (°)	0.44±0.01		0.46±0.01	
Measures of structural quality				
E_{LJ} (kcal mol^{-1})	−772±23		−737±25	
PROCHECK percentage of residues in regions of the Ramachandran plot (for residues with S(ϕ) and S(ψ)≥0.9)				
Most favourable	87.6 (92.4)		90.2 (92.2)	
Additionally allowed	11.9 (7.4)		9.5 (7.8)	
Generously allowed	0.5 (0.2)		0.1 (0)	
Disallowed	0.0 (0)		0.3 (0)	
Angular order				
Residues with $S(\phi)\geq 0.9$	177		173	
Residues with $S(\psi)\geq 0.9$	163		173	
Violations				
Experimental distance constraints >0.2 Å	0		0	
Experimental angle constraints >5°	0		0	
Coordinate precision				
Mean pairwise rmsd (Å)	C^{α}, C, N	All heavy	C^{α}, C, N	All heavy
All residues	2.74±0.48	3.13±0.36	2.30±0.57	2.76±0.40
Regular secondary structure α1–α8, α-BH3	0.73±0.10	1.59±0.11	0.78±0.11	1.65±0.11

increased. In contrast, α3 is almost invariant in disposition in all structures. The distance between the C^{α} atoms of residues H205 at the α2–α3 kink and H233 at the C-terminus of α4 increases from 14.1 Å in unliganded Mcl-1 to 19.4±0.5 Å in the complexes, but the α4–α6 helix crossing angle (30.7±3.1°) is unchanged (Fig. 3a). These values attest to the relatively minor structural adjustments associated with BH3 ligand binding. Although the overall topology is maintained, other pro-survival Bcl-2 proteins undergo greater conformational changes on binding that remodels the groove.[5]

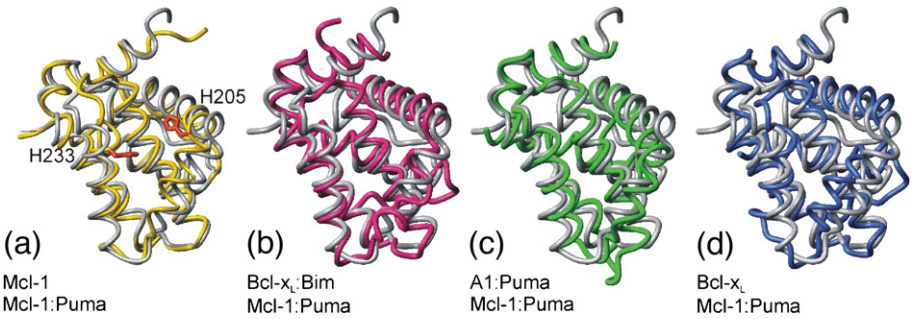

Fig. 3. Comparison of backbone conformations of Mcl-1:Puma with other Bcl-2 proteins. The backbone ribbon of Mcl-1:Puma (PDB code 2ROC) is shown in gray in all panels, and the orientation of the Mcl-1 is the same as that in Fig. 2b. (a) Unliganded Mcl-1 (PDB code 1WSX[15]) in gold. The positions of H205 and H233 are shown. (b) Bcl-x_L:Bim (PDB code 1PQ1[9]) in pink (BH3 ligands not shown). (c) A1:Puma (PDB code 2VOF[19]) in green. (d) Unliganded Bcl-x_L (PDB code 1PQ0[9]) in blue.

Structural comparison of Mcl-1 complexes with other Bcl-2 proteins

Superimpositions of the Mcl-1:Puma structure with those of Bcl-x_L:Bim, A1:Puma and Bcl-x_L are depicted in Fig. 3b–d, and a structure-based sequence alignment of the Mcl-1:Puma complex with Bcl-x_L:Bim and A1:Puma is shown in Fig. 4. Bcl-x_L differs from Mcl-1 and A1 by the presence of a long loop connecting α1 and α2 (Fig. 4) that is absent from the crystal structure[9] and was shown by NMR relaxation studies to be highly mobile.[24] Sequence comparison, excluding loop residues 24–74 of Bcl-x_L and Mcl-1, shows that they share 25.6% identity and 40.0% similarity. The rmsd between Bcl-x_L:Bim and Mcl-1:Puma complexes over the backbone atoms (C^{α}, N, C′) of residues with secondary structure elements common among the complexes of Bcl-x_L, Mcl-1 and A1 (Fig. 4), after structural alignment,[23] is 1.5 Å. In comparison, superposition of unliganded Mcl-1 and Mcl-1:Puma over the backbone atoms gives an rmsd of 1.1 Å when aligned over the shared secondary structural elements. The most notable structural differences between the Mcl-1 complexes and the Bcl-x_L:Bim complex are the changes in location of the helices of the binding groove, as Bcl-x_L only has a single turn of α3 helix, and the little defined secondary structure in this region (Fig. 3b), while Mcl-1 retains this helix on binding (Fig. 3a). A1 and Mcl-1 share 25.4% identity and 46.2% similarity over their helical bundles, have an rmsd of 1.6 Å over the backbone atoms of structurally identical residues and are most similar in their binding profiles. The locations of the groove-defining helices, α3 and α4, are similar in the Puma complexes of Mcl-1 and A1 (Fig. 3c).[19] The main difference between Mcl-1 and unliganded Bcl-x_L (Fig. 3d) is the disposition of helices α3 and α4, in that they are almost parallel in Bcl-x_L and α3 translated towards the N-terminus of helix α5 when compared with the position of α3 in Mcl-1. This results in a closed groove for unliganded Bcl-x_L.[15]

The role of the NWGR motif and BH3 domain binding

Conserved sequence motifs play a role in forming the BH3 binding sites in the pro-survival Bcl-2 family, and one such pattern is the NWGR motif that characterises the BH1 domain. This sequence forms an N-terminal helix-capping motif at the initiation site of helix α5 and is highly conserved in the multi-domain Bcl-2 family including Mcl-1, Bcl-x_L and A1 (Figs. 2 and 4). N-terminal helix-capping motifs arise to satisfy the hydrogen bonding needs of amides in the first turn of helices, and the residues at the initiation site of a helix follow a pattern, …N‴–N″–N′–Ncap–N1–N2–N3…, where the first residue of the helix, N1, is preceded by the N-capping residue, Ncap, and a turn (N‴–N′).[25] Typically, a polar side chain hydrogen bond acceptor, such as serine, threonine, aspartic acid or asparagine, is located in the first four residues, frequently the Ncap residue, and forms hydrogen bonds with the amide donor located at helical position N1–N3.[25] In Mcl-1, the asparagine of the NWGR motif forms the Ncap residue and the side chain carbonyl of this residue is a hydrogen bond acceptor for the amide of arginine at the N3 position (Fig. 5a), while the tryptophan is the first helical residue. In addition to its role as an intramolecular N-capping motif, the NWGR motif also interacts with the ligand BH3 domain, and an intermolecular N-capping interaction is formed between polar residues on the BH3 ligand (e.g., N37 in Fig. 5a) and the N-terminal residues of α5 (G262 in Fig. 5a).

The change in accessible solvent area of Mcl-1 on binding a BH3 ligand is 960±146 $Å^2$, and the site measures about 40×20 Å. Mcl-1 presents a similar surface for BH3 binding in all complexes, with 30%–40% of the BH3 domain binding surface provided by residues conserved among the pro-survival Bcl-2 family.[15] Hydrophobic contacts contribute 40%–50% of the buried surface, and the conserved leucine of Noxa and that of Puma are buried in a hydrophobic pocket that is formed from the side chains of residues

Fig. 4. Sequence and secondary structure comparison of Bcl-2 domains from Mcl-1, Bcl-x_L and A1 complexes. Pairwise structure-based sequence alignment of Mcl-1:Puma (PDB code 2VOF[19]) and Bcl-x_L:Bim (PDB code 1PQ1[9]) using TOP.[23] Coloured bars on the sequence represent the positions of helices α1–α8, underlined are C-terminal deletions and not shown is the N-terminal sequence of Mcl-1. For Mcl-1, the BH1–BH3 domains are shown by the yellow bars above the sequence. The basic patch on Mcl-1 formed by R214 and K215 and the acidic patch by D57 and D58 in A1 are indicated by asterisks.

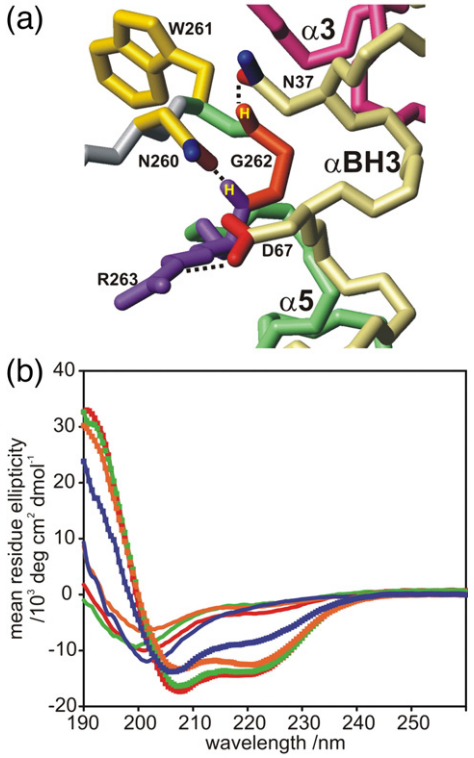

Fig. 5. BH3 domains are unstructured in solution. (a) Detail of NoxaB binding Mcl-1 (PDB code 2NL9[10]) showing the NWGR motif of the BH1 domain α5 and the N-capping interaction. The side chain of N260 forms a hydrogen bond with R263 HN, and an intermolecular N-cap occurs between the side chains of N70 and G262. The BH3 helix is coloured yellow, and the key side chains are illustrated. (b) CD spectra of the BH3 domains for Puma (orange), NoxaA (blue), NoxaB (red) and Bim (green) are shown in the presence (square/line) and in the absence (line only) of 30% trifluoroethanol.

M212, V230, V234, T247 and F251. With the exception of T247, which is substituted for alanine in Bcl-2, Bcl-x_L and Bcl-w, the residues that surround this leucine are either conserved or conservatively substituted across the pro-survival family.[15] On the other hand, Mcl-1 is distinguished from other pro-survival proteins by the presence of a basic patch formed by R214 and K215 in the α3–α4 loop. Acidic residues E136, E32 and E74 from Puma, NoxaA and NoxaB, respectively,[10] (Fig. 1) are in close proximity to K215, and this charge complementarity with Mcl-1 differentiates these three BH3 domains from others.

The consensus BH3 domain binding motif

Circular dichroism (CD) analysis of the BH3 domain peptides in isolation, in contrast to their bound form, showed that the NoxaA, Puma, NoxaB and Bim BH3 domains have CD spectra typical for unstructured peptides (Fig. 5b). In the presence of trifluoroethanol, the helix content increased, demonstrating the helical propensity of these isolated BH3 domains (Fig. 5b).

We performed detailed sequence and structural analyses of BH3 domain pro-survival complexes in order to identify more clearly the features that define this interaction. In addition to contributing four residues that are buried in the hydrophobic pockets of Mcl-1, optimal packing of the BH3 helix in the binding groove may be aided by the presence of two small residues (G, A, S or C, labelled $\dot{\Sigma}$ and $\dot{\Sigma}'$ in Fig. 1) adjacent to the first and third hydrophobic residues. These residues potentially provide a flatter binding surface, a common feature of helical bundle proteins,[26] and T247, or the equivalent alanine in other pro-survival proteins, makes conserved interactions with $\dot{\Sigma}'$ (Fig. 1). Again, the NWGR motif plays a role here, as the $\dot{\Sigma}'$ residue, typically a glycine of the BH3 ligand, packs against the glycine of this BH1 motif. The other small residue ($\dot{\Sigma}$) packs against V230, H233 and V234 on α4 of Mcl-1, and these residues are conservatively substituted in pro-survival proteins. A phylogenetic analysis of BH3 domain-containing proteins suggested the minimal consensus motif LXXXGDE for the BH3 domain.[8] After structural analysis of all BH3 complexes currently available, including those of Mcl-1, a more general 13-residue motif that covers approximately two heptads of the α-helix of the BH3 domain can be described: $\Phi_1\dot{\Sigma}XX\Phi_2XX\Phi_3\dot{\Sigma}'DZ\Phi_4\Gamma$, where Φ represents a hydrophobic residue (Φ_2 is usually leucine); $\dot{\Sigma}$ is a small residue (G, A, S); Z is usually an acidic residue; and Γ is a hydrophilic residue capable of forming the intermolecular N-capping motif (Figs. 1 and 5a). The Γ position of BH3-only proteins is occupied by a hydrophilic residue (N, H, D or Y) and is located immediately after the fourth hydrophobic residue (Fig. 1), and this residue forms an intermolecular N-capping interaction with the glycine residue that occupies the N2 position in the NWGR motif. Proteolysis of Bim bound to Bcl-x_L[9] or Bcl-w[17] gave a peptide fragment that spanned the core 13-residue BH3 region. Collectively, these features define the basis of the interactions that underpin binding of the amphipathic BH3 domains to pro-survival proteins.

Chemical shift perturbation monitoring of Mcl-1 complexes

The sensitivity of the chemical shift to structure and structural change makes it of utility in mapping interaction interfaces and assessing binding.[27] In order to survey the interaction between BH3 ligands and Mcl-1, we undertook a screening approach using chemical shift perturbations in ^1H,^{15}N HSQC spectra as an indicator of binding. If chemical shifts are unperturbed on ligand addition, then the affinity is negligible. By performing a set of titrations and monitoring the positions of HN resonances in a series of ^1H,^{15}N HSQC spectra of Mcl-1, we determined whether there was an interaction with the BH3 domain peptides from mouse Bim, Bid, Bmf as well as Bak, human Noxa and the related BH3-like ligands Mule[28] and Beclin-1.[20] As expected from our binding studies, all ligands except Beclin-1 bound

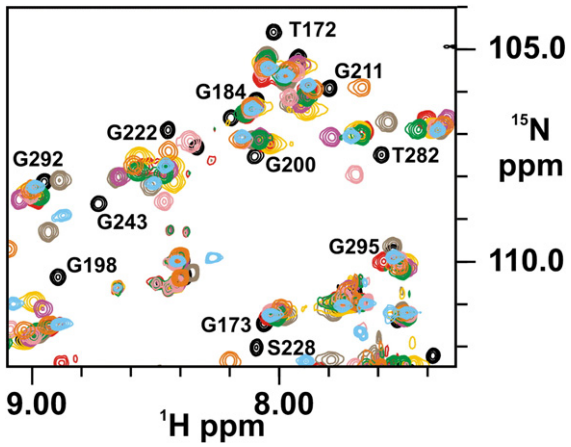

Fig. 6. Comparison of the ^{1}H,^{15}N HSQC spectra of ^{15}N-labelled Mcl-1 in the presence of unlabelled BH3 domain peptides. Superimposed HSQC spectra of Mcl-1 bound to BH3 ligands: unliganded Mcl-1 (black contours); Puma (orange); and Bak (purple). Only the glycine region of the spectrum is shown.

tightly to Mcl-1, on the NMR timescale, while the Beclin-1 BH3 domain left resonances unperturbed, indicating that any affinity for Mcl-1 was extremely weak (Fig. 6 and other data not shown). Although the nature of these data is qualitative, some resonances (e.g., G173) show little or no movement from their position in unliganded Mcl-1, indicating areas of local structural invariance. Many HN resonances common between spectra move upon binding (e.g., T282), indicating that the Mcl-1 structure accommodates each BH3 ligand in a similar manner, as our structural studies show. As a consequence of the lack of sequence conservation between the BH3 domains, the exact atomic interactions between the BH3 and Mcl-1 will be unique, and this in part accounts for the chemical shift differences between the complexes, particularly in the binding groove.

To more fully define the interaction between Mcl-1 and the Bak BH3 domain, we assigned the backbone resonances (C^{α}, N, HN, C′) of Mcl-1 in the presence of one equivalent of the Bak BH3 domain peptide and determined the chemical shift differences between free and bound Mcl-1 for the C^{α} atoms of Mcl-1 (Fig. 7a). The patterns of chemical shift changes induced by binding BH3 domains from mouse NoxaA, NoxaB,[10] Puma and Bak are strikingly similar and indicate that all four ligands induce a similar conformational change in Mcl-1. In the case of the Bak and Puma BH3 domains, chemical shift perturbations greater than |0.5| ppm were plotted on the solvent-accessible surface of Mcl-1 (Fig. 7b and c). The larger chemical shift perturbations are chiefly confined to residues that immediately encircle the binding site. Only small shifts are seen in α3, suggesting that it remains helical, as the chemical shift indices[29] and structures indicate, and is essentially invariant among the complexes. Of the chemical shift differences seen in α3, the largest arises from residue V197, whose side chain projects into the binding interface. The largest chemical shift changes are localised to the C-terminus of α4 that forms part of the binding site and is consistent with α4 moving to accommodate the Bak BH3 domain, as observed in the other complexes (Fig. 3a).

The chemical shift differences for the C^{α} resonances of C-terminal residues differ between the complexes. This region is poorly ordered in Mcl-1, and the C-terminal shift differences observed on NoxaB binding may reflect the more hydrophobic nature of its C-terminus relative to other BH3 domain peptides studied (Fig. 1). Electrostatic effects of the charged BH3 domain C-terminus may also play a role. However, any interaction must be transient in nature, as, consistent with the absence of any stable structural elements, there is no intermolecular NOE in this region. Besides these differences, a number of small chemical shift perturbations occur in resonances derived from residues remote from the binding site. These small perturbations are similar in magnitude,

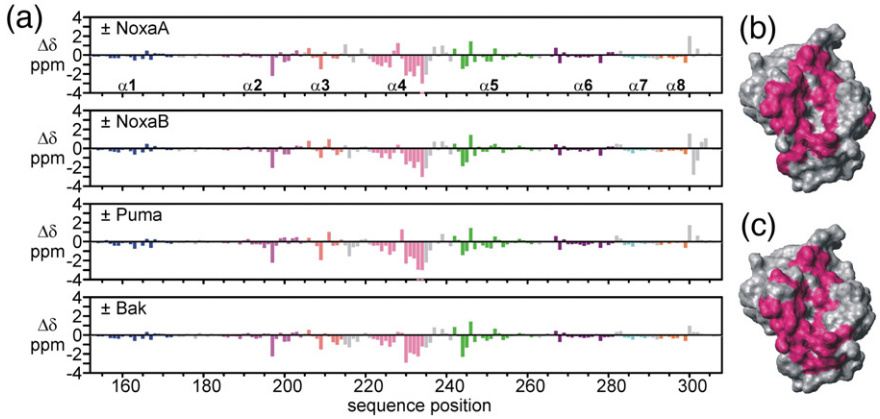

Fig. 7. Chemical shift perturbations of Mcl-1 resonances in the presence of BH3 peptides. (a) Plot of chemical shift differences between free and bound Mcl-1 for NoxaA, NoxaB, Puma and Bak complexes. The secondary structure is indicated by the colours of the bars. (b) Chemical shift perturbations for Bak BH3 binding displayed on the solvent-accessible surface of Mcl-1. (c) Chemical shift perturbations for Puma on the Mcl-1 surface in the Puma complex. In (b) and (c), chemical shift differences >|0.5| ppm are displayed in magenta. The view is identical with that for the ribbon in Fig. 3.

Table 2. Thermodynamic parameters for BH3 domain peptides binding Mcl-1 determined by ITC at 25 °C

BH3	K_d (nM)	ΔH (kcal mol^{-1})	ΔS (cal mol^{-1} K^{-1})
NoxaA	39.5	−20.7	−35.5
NoxaB	126.0	−32.6	−77.9
LNoxaB	72.5	−23.6	−46.6
NoxaB E74F	73.0	−20.2	−34.9
Puma	1.8	−24.5	−42.3
Puma M144I	0.69	−14.3	−5.9
Bmf	328.9	−11.5	−8.9
Bak	2.6	−22.1	−34.8
Bim	2.10	−19.2	−24.1
Bid (34-mer)	9.8	−17.5	−21.9

Details of the peptides are given in Materials and Methods.

sign in all complexes and point to small conformational changes in the helical bundle to accommodate the ligand. Together, the chemical shift differences indicate that similar contacts mediate interactions between all BH3 peptides and Mcl-1.

Mcl-1 binding selectivity

We determined the binding constants for peptides that span the BH3 domains of BH3-only proteins for Mcl-1 by isothermal titration calorimetry (ITC); the thermodynamic parameters are given in Table 2. Typical ITC curves are plotted in Fig. 8a, and the entropy–enthalpy plot in Fig. 8b illustrates that there is a strong degree of entropy–enthalpy compensation for binding of the BH3 domain ligands to Mcl-1. The points were fitted using linear regression, giving a line of slope of 0.93 and a regression coefficient, R^2, of 0.96. Entropy–enthalpy compensation is common in protein–ligand interactions and has the effect of minimising the variation in the free energy of binding by balancing the entropic and enthalpic contributions.[30] The origins of this effect lie in the adjustments of non-covalent interactions in the receptor-to-ligand binding[31] and contributions from solvent reorganisation.[32]

The K_d values for BH3 domain binding Mcl-1 span approximately 3 orders of magnitude, and the universal pro-survival protein binders Bim, Puma and the Puma mutant Puma M144I bind Mcl-1 with high affinity (K_d values of 2.1, 1.8 and 0.69 nM, respectively). Bmf, on the other hand, has a comparatively low affinity, with an observed K_d of 329 nM, making it uncertain if this protein initiates apoptosis by binding Mcl-1.

Each Noxa BH3 domain has a distinct binding profile. Mcl-1 binds both NoxaA and NoxaB, although NoxaA has a 3.2-fold greater affinity for Mcl-1, but it is still 19-fold lower than for Bim and 22-fold lower than for Puma. In contrast, A1 binds NoxaA, but its interaction with NoxaB is not detectable by surface plasmon resonance (SPR).[11] NoxaA and NoxaB have different sequences, and a phenylalanine residue in NoxaA occupies the first conserved hydrophobic residue, Φ_1, that is replaced by a glutamate in NoxaB (Fig. 1). The NoxaB mutation E74F improves its affinity 1.7-fold for Mcl-1, and this BH3 domain now binds A1. The human Noxa peptide (Fig. 1) binds both A1 and Mcl-1 and behaves more like NoxaA.[11] The presence of two BH3 domains with distinct binding profiles in mouse Noxa differentiates it from other species and potentially allows it to control different signalling pathways. Notably, inactivation of A1 in the mouse may be of increased significance as there are four A1 variants in the mouse genome.[33] Analysis by SPR showed that A1 binds NoxaB E74F with an IC_{50} of 24 nM and that Mcl-1 does with an IC_{50} of 11 nM.

Mapping the Mcl-1 binding site on Noxa by phage display

In order to determine the contribution of individual residues to binding, we probed the Mcl-1: NoxaA interaction by alanine scanning the BH3 domain of NoxaA using phage display. These studies indicate that only residues (L27, I30, G31,

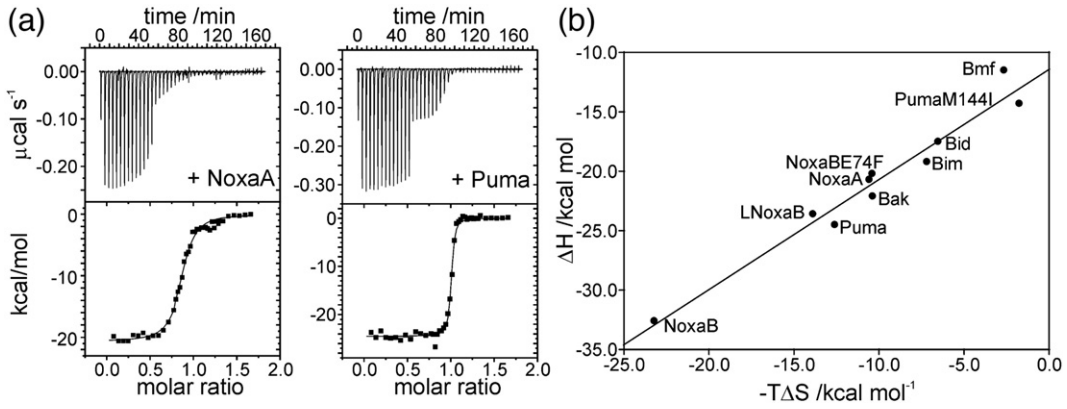

Fig. 8. Isothermal titration calorimetric measurements for Mcl-1 BH3 domain complexes at 25 °C. (a) ITC titration for PumaBH3, corresponding to a K_d of 1.8 nM. (b) NoxaA BH3 binding Mcl-1, corresponding to a K_d of 39.5 nM. The details of the titrations are given in Materials and Methods and Table 2. The step in the injection profile arises from a reduction of the injection volume close to the inflection point of the binding curve for greater accuracy. (b) Entropy–enthalpy compensation is demonstrated for Mcl-1 BH3 domain binding by the plot of ΔH *versus* $-T\Delta S$ (Table 2).

D32 and V34) within, or immediately adjacent to, the central LXXXGDE sequence (for Noxa, Glu is substituted by Lys in this sequence; see Fig. 1) of the BH3 domain are critical (Fig. 9). A separate assay using an anti-FLAG antibody confirmed that the low signal was not due to poor expression (data not shown). The contribution of individual residues was also demonstrated using synthetic peptides. Each mutant tested in solution competition assays using SPR gave IC_{50} values significantly lower than the IC_{50} value obtained for the wild-type mouse NoxaA sequence (Fig. 9b). Importantly, the IC_{50} of the wild-type peptide sequence was almost identical with that obtained using phage display (42 *versus* 39 nM). Surprisingly, replacement of the phenylalanine F23, a residue that binds in the first binding pocket of Mcl-1, with alanine did not affect binding significantly. This contrasts with the observations of Sattler *et al.*, in which the spatially equivalent residue in Bak BH3 (V81) was shown to be important for binding Bcl-x_L.[7] Together with the results of Czabotar *et al.*,[10] these data indicate that interaction of NoxaB with Mcl-1 depends on the central region of the BH3 domain, as deletion of five N-terminal residues from NoxaB had little effect on binding. Likewise, NoxaB with seven additional C-terminal residues, potentially two turns of helix, bound to Mcl-1 with approximately the same affinity (K_d values of 126 and 58 nM for NoxaB and long NoxaB, respectively; Table 2).

The strong effect seen in the phage assays following substitution of G31 to glutamic acid probably arises from a combination of steric and electronic effects occurring from the need to bury a larger charged residue. This residue of the BH3-only protein is normally buried packing against the conserved glycine in the NWGR motif of the BH1 domain of the pro-survival protein.

Discussion

Apoptotic signalling pathways that proceed through mitochondria are critically dependent on the interaction between BH3-only proteins and their pro-survival Bcl-2 counterparts.[1] Each BH3-only protein is able to bind multiple pro-survival Bcl-2 proteins, and while some (e.g., Bim, Bid, Puma) bind all pro-survival members with approximately equal affinity, others have a more defined specificity, binding only subsets of these proteins (e.g., Noxa).[11] To help unravel the molecular basis of these interactions, we determined the structure, binding and thermodynamic properties of the interactions between the pro-survival Bcl-2 family member Mcl-1 and the binding domains of BH3-only proteins Noxa and Puma.

Structures of Puma and Noxa bound to Mcl-1

Although in isolation the Puma and NoxaA BH3 peptides are unstructured in solution, when bound to Mcl-1, they form well-ordered α-helices that pack in a hydrophobic groove formed in part by the BH1–BH3 domains and residues located on helices α2–α5 and α8 of Mcl-1 (Figs. 2, 3 and 7). The NoxaA and Puma BH3 peptides provide approximately 1000 $Å^2$ of buried surface area in the Mcl-1:BH3 interface, while the total accessible solvent area buried on forming the complex is about 2000 $Å^2$, values typical of non-obligate protein complexes.[34] The 'helix-in-groove' mode of binding of NoxaA and Puma is similar to that of other pro-survival BH3 complexes,[7,9,10] and the conserved 'anchor residue'[35] leucine, together with other hydrophobic residues, forms one face of an amphipathic BH3 helix that is buried in a tightly packed interface. On the periphery of the groove, polar and ionic residues of the BH3 domain contribute to binding interactions. Such solvent-accessible interactions are maintained among the Mcl-1 complexes; for example, Puma, NoxaA and NoxaB[10] have acidic groups located at the N-terminal end of the BH3 domain (Fig. 1) that lie in close proximity to a basic patch provided by R214 and K215 on the surface of Mcl-1.

Mcl-1 undergoes minimal conformational change on binding

The pro-survival protein undergoes structural transition on binding. Chemical shift deviations between unliganded and liganded Mcl-1 showed that all ligands perturb Mcl-1 backbone resonances in a similar way and indicated that each ligand gives rise to similar conformational changes in Mcl-1 on binding (Figs. 6 and 7). Small but consistent chemical

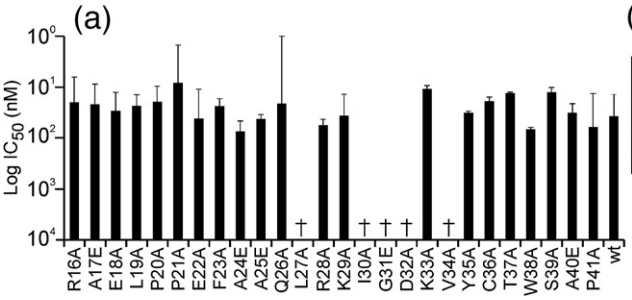

mNoxaA	IC_{50} (nM)
wild-type	42
L27A	> 25,000
I30A	> 25,000
D32A	> 25,000
V34A	9,500

Fig. 9. Binding affinities of mNoxaA mutants. (a) The affinities of phage-displayed mouse NoxaA BH3 domain and NoxaA BH3 mutants were measured in a solution competition assay. Mutants indicated with a cross are those that bound too weakly in an initial phage titration to allow an accurate IC_{50} to be determined. The error bars indicate the standard deviation from the mean of $n = 2$ assays. (b) Synthetic peptides corresponding to most of the weak binding sequences identified in the phage assays were tested in competition assays using SPR. All bound with affinities significantly lower than those for the wild-type peptide.

shift differences occur outside the direct binding residues, indicating conformational changes in the helical bundle on accepting a ligand. Irrespective of the BH3 ligand, these resonance changes occur in similar regions of the helical bundle in each case (Fig. 7a), indicating only relatively minor differences in the binding modes of BH3-bearing proteins.

Structural comparison with other Bcl-2 family members and their complexes

The most striking structural difference between the BH3 complexes of Mcl-1 and Bcl-x_L and their unliganded forms is the behaviour of residues in α3 and α4, which flank the groove and provide contact residues for the ligand.[15] In Bcl-x_L, α4 undergoes a rotation to alter the α4–α6 helix crossing angle from 60° to be almost parallel with α6, and the residues of α3 become less ordered on binding (Fig. 3). These ligand-induced changes in Bcl-x_L have the effect of developing the binding site by exposing residues that are buried in the closed conformation and creating space for the ligand. In contrast, α3 of Mcl-1 is essentially unperturbed on ligand binding (Fig. 2), and while α4 undergoes a translation to widen the groove, the movement of α4 in Bcl-x_L is larger. One caveat for these conformational changes in pro-survival Bcl-2 proteins is that only C-terminally truncated molecules have had their structures determined. It has been shown with Bcl-w that the C-terminal tail lies in the groove in a reverse orientation to the BH3 ligand.[36] Functional studies on Bcl-x_L and Bcl-w[36] and binding studies on Mcl-1[15] indicated that the C-terminal residues slow access to the binding groove but do not prevent BH3 binding. The significance of the conformational change in the α3 and α4 helices of C-terminally truncated Bcl-x_L[9] is therefore unclear. However, it is apparent that the helical bundles of the pro-survival proteins are dynamic and structural transitions of the pro-survival proteins are important in their binding interactions.

The BH1 and BH3 motifs: partners in binding

Pro-apoptotic proteins are defined by the presence of a BH3 domain.[3] BH3 domains bear conserved leucine and aspartic acid residues in a simple sequence motif, LXXXGDE,[8] although neither the Gly nor the Glu residues are strictly conserved (Fig. 1). We noted earlier the presence of four hydrophobic groups,[11] Φ_1–Φ_4, that are spaced to form the hydrophobic face on a BH3 helix. However, again, there is no strict conservation, as the first hydrophobic residue, Φ_1, is replaced by an acidic (Glu) residue in NoxaA (Fig. 1). Key binding interactions occur between the BH3 ligand and the BH1 domain of the pro-survival protein. The multi-BH domain Bcl-2 proteins, including Mcl-1, bear an NWGR sequence motif that defines the initiation site of helix α5 and forms a helix-capping motif, with the side chain carbonyl of the asparagine hydrogen bonded to the arginine amide. The arginine of the NWGR sequence forms a key polar interaction with the aspartate of the BH3-only ligands; an intermolecular hydrogen bond with the side chain of a residue C-terminal to the fourth hydrophobic residue (Γ and Φ_4 in Fig. 1, respectively) of the ligand fulfils the hydrogen bonding needs of the glycine. Two small residues (Σ, Σ′) separated by a heptad, and therefore on the same face of a helix, are required for tight packing of the helical BH3 domain into the groove of the pro-survival protein. Together, these structural and sequence analyses suggest a more accurate generalised motif for BH3 domains that is composed of 13 residues, $\Phi_1\Sigma XX\Phi_2XX\Phi_3\Sigma'DZ\Phi_4\Gamma$.

Binding characteristics of Noxa and Puma with Mcl-1

In order to understand the contributions of individual residues to binding to Mcl-1, we performed a mutational analysis of NoxaA using alanine scanning. Interestingly, although the NoxaA alanine scan showed substantial reduction in affinity when the key BH3 leucine was replaced by alanine (>25,000-fold reduction over wild-type NoxaA; Fig. 9b), truncation of the BH3 domain N-terminus by five residues[10] or extension of the C-terminus of NoxaB BH3 had relatively little effect on binding (Table 2), consistent with the relative insensitivity of binding to mutations outside the core $\Phi_2XX\Phi_3\Sigma'DZ\Phi_4$ region of the BH3 domain (Fig. 9). These observations echo those of Lee *et al.*,[37] who showed that the conserved leucine (Φ_2) of Bim could be replaced with any residue, except a charged residue, and retain measurable Mcl-1 binding and that mutation of Φ_4 had little effect. In contrast, although Bcl-x_L could bind a variety of Bim mutants tightly, it was more sensitive to residue type; however, Bim binding may be less sensitive than Noxa to point mutations due to its inherently higher binding affinity.

The two BH3 domains of mouse Noxa, NoxaA and NoxaB (Fig. 1), differ at the first hydrophobic residue, Φ_1, and consistent with the decreased significance of this position, NoxaB, which bears an acidic residue at this position (E74), binds Mcl-1 with only threefold lower affinity than NoxaA, which has a hydrophobic residue (F23). The NoxaB mutant NoxaB E74F gained affinity for Mcl-1 by less than twofold (Table 2). Structurally, the two Noxa BH3 peptides bind in slightly different modes; in the Mcl-1:NoxaB complex, E74 is in close proximity to a basic patch (R214 and K215 as outlined above) unique to Mcl-1, while in the Mcl-1:NoxaA complex, F23 of NoxaA folds away from the basic patch and makes hydrophobic contacts.[10] The basic patch could be potentially used by other BH3 domains, such as Mule, which has an acidic residue at the appropriate sequence position, while others, such as Bad and Hrk, cannot make the same interaction. Interestingly, NoxaA but not NoxaB binds A1, and in contrast to Mcl-1, A1 has an acidic patch provided by two aspartates (D57 and D58) in a position structurally equivalent to the basic patch on Mcl-1 (Fig. 4).[19] The A1 acidic patch would potentially make unfavourable contacts with E74 in NoxaB, and,

notably, the NoxaB E74F mutant gains affinity for A1. Together, these results show that the Φ_1 residue has reduced significance for Mcl-1 and that this residue may act as a selectivity filter, differentiating Mcl-1 from other pro-survival Bcl-2 proteins.

BH3 binding thermodynamics

Despite being unstructured in solution, the BH3-only peptides can bind tightly to Mcl-1, with affinities down to, or below, the 1 nM range (Table 2). As might be expected for proteins that bind in a hydrophobic groove, the entropic contribution to the free energy for BH3 domain binding Mcl-1 is unfavourable and, although both binding partners undergo conformational change, the association is exothermic as well as being strongly entropy–enthalpy compensated. These features place BH3 binding among other protein–protein interactions in which the free energy of binding is typically dominated by the enthalpic contribution.[18] Entropy–enthalpy compensation has been linked to the rearrangement of internal non-covalent interactions of the protein on binding, and Williams *et al*. proposed that a 'structural tightening' is associated with a positively cooperative binding and a 'loosening' is associated with a negatively cooperative process.[31] Such a mechanism would predict long-range chemical shift changes that we observe with Mcl-1 on ligand binding. The importance of contributions from receptor dynamics and conformational entropy to binding interactions has been demonstrated for calmodulin, which, like Mcl-1, binds a number of peptide targets as helices.[38] A significant redistribution of the fast side chain dynamics in calmodulin occurs on ligand binding,[39] and this change in internal protein dynamics makes a significant contribution to the free energy of binding and formation of high-affinity interactions.[38] Furthermore, the internal dynamics of peptide-bound calmodulin is highly ligand dependent and varies considerably with the ligand, suggesting that alteration in internal conformational entropy tunes the ligand affinity.[38] Together, these results are consistent with our findings for Mcl-1, as the BH3 ligand binds to form a compact α-helix and resonance positions in $^{1}H,^{15}N$ HSQC spectra are altered for amides remote from the binding site.

Biological relevance and conclusions

Breakdown in apoptosis regulation is a common feature in cancer and is frequently characterised by loss of p53 regulation of Bcl-2 proteins.[40] In turn, overexpression of pro-survival proteins, such as Mcl-1, prevents cells from responding appropriately to apoptosis-promoting molecules as Noxa and Puma. Defining the specificity and key interactions of BH3-only proteins for their targets not only is necessary to describe the apoptotic pathways that they signal but also may have practical application in the design of new cancer therapeutics that target specific Bcl-2 family members.[16] Current approaches using BH3 mimetics to neutralise pro-survival Bcl-2 proteins to initiate apoptosis in cancer cells only target Bcl-2, Bcl-x_L and Bcl-w,[41] and cells that are dependent on Mcl-1 for survival are resistant to treatment.[42] NoxaB BH3 specifically targets Mcl-1 and exploits a basic patch unique to the Mcl-1 sequence; also, in the mouse, it suggests that Noxa, with its two BH3 domains, may have unique signalling pathways through A1 and Mcl-1. Exploiting the unique molecular features of Mcl-1, as demonstrated by its interaction with NoxaB, may provide a means to design specific inhibitors for Mcl-1.

The structures of Mcl-1 in complex with the NoxaA and Puma BH3 domains presented here elucidate features important for Mcl-1 binding to BH3-only antagonists. A core 13-residue motif accounts for the BH3 domain binding interactions, and we also show that the binding energetics of these unstructured BH3 domains conforms to that typical of other protein–protein interactions. Although van der Waals and hydrophobic forces are the dominant interactions between IUPs, such as the BH3-only proteins, and their receptors,[43–45] we showed that polar interactions play an important role in determining binding and specificity of these proteins.

Materials and Methods

Expression and purification of proteins

Mouse Mcl-1 (accession number AA31790) with 151 N-terminal residues and 23 C-terminal residues truncated, Mcl-1ΔNC23, was expressed as a glutathione *S*-transferase fusion protein in *Escherichia coli* BL21(DE3) and purified as described previously.[15] Mouse NoxaA and Puma BH3 domain peptides [NoxaABH3: residues 16–42 of mouse Noxa (sequence AELPPEFAAQLRKIGDKVYCTWSAPD), accession number NP_067426; PumaBH3: residues 130–155 of mouse Puma M144I (sequence EEEWAREIGAQLRRIADDLNAQYERR),[19] accession number NM_133234] were prepared using the pET-31b expression vector (Novagen) as outlined previously.[17] Mass spectrometry was used to confirm peptide homogeneity. Isotopically labelled proteins were prepared by growth in minimal media using $^{15}NH_4Cl$ and U^{13}C D-glucose as the sole nitrogen and carbon sources, respectively, as previously described.[46] BH3 complexes were prepared by titration using NMR to detect the end point. For each structure, two samples were prepared, $^{13}C,^{15}N$-labelled Mcl-1/unlabelled BH3 peptide and unlabelled Mcl-1/$^{13}C,^{15}N$-labelled BH3 peptide. NMR samples contained ~0.5 mM protein in 50 mM sodium phosphate, pH 6.7, 70 mM NaCl and 0.04% sodium azide in H_2O:$^{2}H_2O$ (95:5).

NMR spectroscopy and spectral assignments

Spectra were recorded at 25 °C on a Bruker DRX 600 spectrometer equipped with triple-resonance probes and pulsed-field gradients operating at 600 MHz or with AV-500 and AV-800 spectrometers equipped with cryogenically cooled probes operating at 500 and 800 MHz, respectively. A series of heteronuclear three-dimensional NMR experiments was recorded using either ^{15}N- or $^{13}C,^{15}N$-doubly labelled Mcl-1ΔNC23.[21] Spectra were processed using TOPSPIN (Bruker AG) and analysed using XEASY.[47]

Distance and dihedral angle restraints

Distance restraints were measured from the 120-ms-mixing-time three-dimensional ^{15}N-edited nuclear Overhauser enhancement spectroscopy (NOESY), ^{13}C-edited NOESY and two-dimensional NOESY spectra. Hydrogen bond constraints were applied within α-helices at a late stage of the structure calculation.[36] ϕ and ψ backbone torsion angles were derived using TALOS.[48] Dihedral angle restraints for ϕ and ψ angles were used as summarised in Table 1. $^{3}J_{HNH}\alpha$ constants were derived from a three-dimensional HNHA spectrum.[49]

Structure calculation and analysis

Initial structures were calculated using CYANA 2.1,[50] optimised to obtain low target functions and then refined with Xplor-NIH 2.14[51] using the OPLSX non-bonded parameters in explicit water.[52] Structural statistics for the final set of 20 structures, chosen on the basis of their stereochemical energies, are presented in Table 1. PROCHECK_NMR[22] and MOLMOL[53] were used for the analysis of structure quality. The final structures had no experimental distance violation greater than 0.2 Å or dihedral angle violation greater than 5°. Structure superimposition was based on residues chosen with the program TOP.[23] Structural figures were generated in MOLMOL.[53]

Binding studies

Binding constants were determined using ITC. Experiments were performed using a VP-ITC (MicroCal). BH3 domain peptides were dissolved at between 1–3 mM in water and quantitated using the absorbance at 205 nm. Mcl-1 was dialysed into phosphate buffered saline (PBS) and quantitated using the absorbance at 280 nm. The peptides were diluted to the desired concentration using PBS, while Mcl-1 was diluted using PBS and water to match the peptide buffer. For weakly interacting ligands, Mcl-1 was diluted to 10 μM and the BH3 domain peptide was diluted to 120 μM with 10-μL injections of peptide. In the case of high-affinity interactions, Mcl-1 was diluted to 5 μM and the peptide was diluted to 40 μM, and two injection volumes were used to obtain more points during saturation. Injections of 10 μL were used, except for a ligand stoichiometry of 0.8–1.2, in which 4-μL injections were used. The data were analysed using Origin and fitted to a single-site binding model. SPR analyses of A1 and Mcl-1 were performed according to earlier methods.[11]

Solution competition assays

Solution competition assays using the Biacore optical biosensor were performed as described previously,[11] using synthetic BH3 peptides (Mimotopes) based on the wild-type mouse Noxa BH3 sequence (amino acids 16–41: RAELPPEFAAQLRKIGDKVYCTWSAP) and 10 nM mouse Mcl-1ΔN151ΔC23. For the phage binding assays, the wild-type Noxa BH3 domain 26-mer (as above) and mutants were displayed as FLAG-tagged fusions to gene 3p on M13 phage, as previously described for other BH3 sequences.[37] Phage particles were then tested at a subsaturating dilution in a solution competition ELISA, in which soluble mouse Mcl-1ΔN151ΔC23 was used to compete phage-displayed Noxa BH3 from binding to Mcl-1 immobilised on a 96-well plate (Nunc). Binding was determined by using a horseradish peroxidase-labelled anti-M13 antibody. A corresponding titration ELISA using an anti-FLAG antibody was also performed to ensure adequate expression of all mutants.

PDB accession codes

Atomic coordinates and experimental constraints have been deposited in the PDB: Mcl-1:Puma with PDB code 2ROC and Mcl-1:NoxaA with PDB code 2ROD.

Acknowledgements

NMR spectra were acquired at the Bio21 Institute NMR Facility of the University of Melbourne. Our research was supported by the Marsden Fund (New Zealand), the Leukemia and Lymphoma Society (Specialized Center for Research, grant no. 7015-02) and the Australian National Health and Medical Research Council (program grant no. 257502). We thank Rayleen Fredericks-Short for technical assistance.

References

1. Youle, R. J. & Strasser, A. (2008). The BCL-2 protein family: opposing activities that mediate cell death. *Nat. Rev. Mol. Cell Biol.* **9**, 47–59.
2. Adams, J. M. & Cory, S. (2007). Bcl-2-regulated apoptosis: mechanism and therapeutic potential. *Curr. Opin. Immunol.* **19**, 488–496.
3. Huang, D. C. S. & Strasser, A. (2000). BH3-only proteins—essential initiators of apoptotic cell death. *Cell*, **103**, 839–842.
4. Petros, A. M., Olejniczak, E. T. & Fesik, S. W. (2004). Structural biology of the Bcl-2 family of proteins. *Biochim. Biophys. Acta*, **1644**, 83–94.
5. Hinds, M. G. & Day, C. L. (2005). Regulation of apoptosis: uncovering the binding determinants. *Curr. Opin. Struct. Biol.* **15**, 690–699.
6. van Delft, M. F. & Huang, D. C. (2006). How the Bcl-2 family of proteins interact to regulate apoptosis. *Cell Res.* **16**, 203–213.
7. Sattler, M., Liang, H., Nettesheim, D., Meadows, R. P., Harlan, J. E., Eberstadt, M. *et al.* (1997). Structure of Bcl-x_L–Bak peptide complex: recognition between regulators of apoptosis. *Science*, **275**, 983–986.
8. Lanave, C., Santamaria, M. & Saccone, C. (2004). Comparative genomics: the evolutionary history of the Bcl-2 family. *Gene*, **333**, 71–79.
9. Liu, X., Dai, S., Zhu, Y., Marrack, P. & Kappler, J. W. (2003). The structure of a Bcl-x_L/Bim fragment complex: implications for Bim function. *Immunity*, **19**, 341–352.
10. Czabotar, P. E., Lee, E. F., van Delft, M. F., Day, C. L., Smith, B. J., Huang, D. C. S. *et al.* (2007). Structural insights into the degradation of Mcl-1 induced by BH3 domains. *Proc. Natl. Acad. Sci. USA*, **104**, 6217–6222.
11. Chen, L., Willis, S. N., Wei, A., Smith, B. J., Fletcher, J. I., Hinds, M. G. *et al.* (2005). Differential targeting of prosurvival Bcl-2 proteins by their BH3-only ligands allows complementary apoptotic function. *Mol. Cell*, **17**, 393–403.
12. Craig, R. W. (2002). MCL1 provides a window on the role of the BCL2 family in cell proliferation,

differentiation and tumorigenesis. *Leukemia*, **16**, 444–454.
13. Rinkenberger, J. L., Horning, S., Klocke, B., Roth, K. & Korsmeyer, S. J. (2000). Mcl-1 deficiency results in peri-implantation embryonic lethality. *Genes Dev.* **14**, 23–27.
14. Opferman, J. T., Letai, A., Beard, C., Sorcinelli, M. D., Ong, C. C. & Korsmeyer, S. J. (2003). Development and maintenance of B and T lymphocytes requires antiapoptotic MCL-1. *Nature*, **426**, 671–676.
15. Day, C. L., Chen, L., Richardson, S. J., Harrison, P. J., Huang, D. C. S. & Hinds, M. G. (2005). Solution structure of prosurvival Mcl-1 and characterization of its binding by proapoptotic BH3-only ligands. *J. Biol. Chem.* **280**, 4738–4744.
16. Fesik, S. W. (2005). Promoting apoptosis as a strategy for cancer drug discovery. *Nat. Rev. Cancer*, **5**, 876–885.
17. Hinds, M. G., Smits, C., Fredericks-Short, R., Risk, J. M., Bailey, M., Huang, D. C. S. & Day, C. L. (2007). Bim, Bad and Bmf: intrinsically unstructured BH3-only proteins that undergo a localized conformational change upon binding to prosurvival Bcl-2 targets. *Cell Death Differ.* **14**, 128–136.
18. Ross, P. D. & Subramanian, S. (1981). Thermodynamics of protein association reactions: forces contributing to stability. *Biochemistry*, **20**, 3096–3102.
19. Smits, C., Czabotar, P. E., Hinds, M. G. & Day, C. L. (2008). Structural plasticity underpins promiscuous binding of the pro-survival protein A1. *Structure*, **16**, 818–829.
20. Oberstein, A., Jeffrey, P. D. & Shi, Y. (2007). Crystal structure of the Bcl-x_L–Beclin 1 peptide complex: Beclin 1 is a novel BH3-only protein. *J. Biol. Chem.* **282**, 13123–13132.
21. Sattler, M., Schleucher, J. & Griesinger, C. (1999). Heteronuclear multidimensional NMR experiments for the structure determination of proteins in solution employing pulsed field gradients. *Prog. Nucl. Magn. Reson. Spectrosc.* **34**, 93–158.
22. Laskowski, R. A., Rullmann, J. A. C., MacArthur, M. W., Kaptein, R. & Thornton, J. M. (1996). AQUA and PROCHECK-NMR: programs for checking the quality of protein structures solved by NMR. *J. Biomol. NMR*, **8**, 477–486.
23. Lu, G. G. (2000). TOP: a new method for protein structure comparisons and similarity searches. *J. Appl. Crystallogr.* **33**, 176–183.
24. Muchmore, S. W., Sattler, M., Liang, H., Meadows, R. P., Harlan, J. E., Yoon, H. S. *et al.* (1996). X-ray and NMR structure of human Bcl-x_L, an inhibitor of programmed cell death. *Nature*, **381**, 335–341.
25. Aurora, R. & Rose, G. D. (1998). Helix capping. *Protein Sci.* **7**, 21–38.
26. Gimpelev, M., Forrest, L. R., Murray, D. & Honig, B. (2004). Helical packing patterns in membrane and soluble proteins. *Biophys. J.* **87**, 4075–4086.
27. Zuiderweg, E. R. (2002). Mapping protein–protein interactions in solution by NMR spectroscopy. *Biochemistry*, **41**, 1–7.
28. Zhong, Q., Gao, W., Du, F. & Wang, X. (2005). Mule/ARF-BP1, a BH3-only E3 ubiquitin ligase, catalyzes the polyubiquitination of Mcl-1 and regulates apoptosis. *Cell*, **121**, 1085–1095.
29. Wishart, D. S. & Case, D. A. (2001). Use of chemical shifts in macromolecular structure determination. *Methods Enzymol.* **338**, 3–34.
30. Williams, D. H., Stephens, E., O'Brien, D. P. & Zhou, M. (2004). Understanding noncovalent interactions: ligand binding energy and catalytic efficiency from ligand-induced reductions in motion within receptors and enzymes. *Angew. Chem., Int. Ed. Engl.* **43**, 6596–6616.
31. Williams, D. H., O'Brien, D. P., Sandercock, A. M. & Stephens, E. (2004). Order changes within receptor systems upon ligand binding: receptor tightening/oligomerisation and the interpretation of binding parameters. *J. Mol. Biol.* **340**, 373–383.
32. Leung, D. H., Bergman, R. G. & Raymond, K. N. (2008). Enthalpy–entropy compensation reveals solvent reorganization as a driving force for supramolecular encapsulation in water. *J. Am. Chem. Soc.* **130**, 2798–2805.
33. Hatakeyama, S., Hamasaki, A., Negishi, I., Loh, D. Y., Sendo, F. & Nakayama, K. (1998). Multiple gene duplication and expression of mouse *bcl-2*-related genes, A1. *Int. Immunol.* **10**, 631–637.
34. Jones, S. & Thornton, J. M. (1996). Principles of protein–protein interactions. *Proc. Natl. Acad. Sci. USA*, **93**, 13–20.
35. Rajamani, D., Thiel, S., Vajda, S. & Camacho, C. J. (2004). Anchor residues in protein–protein interactions. *Proc. Natl Acad. Sci. USA.* **101**, 11287–11292.
36. Hinds, M. G., Lackmann, M., Skea, G. L., Harrison, P. J., Huang, D. C. S. & Day, C. L. (2003). The structure of Bcl-w reveals a role for the C-terminal residues in modulating biological activity. *EMBO J.* **22**, 1497–1507.
37. Lee, E. F., Czabotar, P. E., Smith, B. J., Deshayes, K., Zobel, K., Colman, P. M. & Fairlie, W. D. (2007). Crystal structure of ABT-737 complexed with Bcl-x_L: implications for selectivity of antagonists of the Bcl-2 family. *Cell Death Differ.* **14**, 1711–1713.
38. Frederick, K. K., Marlow, M. S., Valentine, K. G. & Wand, A. J. (2007). Conformational entropy in molecular recognition by proteins. *Nature*, **448**, 325–329.
39. Lee, A. L., Kinnear, S. A. & Wand, A. J. (2000). Redistribution and loss of side chain entropy upon formation of a calmodulin–peptide complex. *Nat. Struct. Biol.* **7**, 72–77.
40. Hanahan, D. & Weinberg, R. A. (2000). The hallmarks of cancer. *Cell*, **100**, 57–70.
41. Oltersdorf, T., Elmore, S. W., Shoemaker, A. R., Armstrong, R. C., Augeri, D. J., Belli, B. A. *et al.* (2005). An inhibitor of Bcl-2 family proteins induces regression of solid tumours. *Nature*, **435**, 677–681.
42. van Delft, M. F., Wei, A. H., Mason, K. D., Vandenberg, C. J., Chen, L., Czabotar, P. E. *et al.* (2006). The BH3 mimetic ABT-737 targets selective Bcl-2 proteins and efficiently induces apoptosis via Bak/Bax if Mcl-1 is neutralized. *Cancer Cell*, **10**, 389–399.
43. Meszaros, B., Tompa, P., Simon, I. & Dosztanyi, Z. (2007). Molecular principles of the interactions of disordered proteins. *J. Mol. Biol.* **372**, 549–561.
44. Gunasekaran, K. & Nussinov, R. (2007). How different are structurally flexible and rigid binding sites? Sequence and structural features discriminating proteins that do and do not undergo conformational change upon ligand binding. *J. Mol. Biol.* **365**, 257–273.
45. Vacic, V., Oldfield, C. J., Mohan, A., Radivojac, P., Cortese, M. S., Uversky, V. N. & Dunker, A. K. (2007). Characterization of molecular recognition features, MoRFs, and their binding partners. *J. Proteome Res.* **6**, 2351–2366.
46. Day, C. L., Dupont, C., Lackmann, M., Vaux, D. L. & Hinds, M. G. (1999). Solution structure and mutagenesis of the caspase recruitment domain (CARD) from Apaf-1. *Cell Death Differ.* **6**, 1125–1132.
47. Bartels, C., Xia, T. H., Billeter, M., Güntert, P. & Wüthrich, K. (1995). The program XEASY for

computer-supported NMR spectral analysis of biological macromolecules. *J. Biomol. NMR*, **6**, 1–10.
48. Cornilescu, G., Delaglio, F. & Bax, A. (1999). Protein backbone angle restraints from searching a database for chemical shift and sequence homology. *J. Biomol. NMR*, **13**, 289–302.
49. Vuister, G. W. & Bax, A. (1993). Quantitative J correlation: a new approach for measuring homonuclear three-bond J(HNHα) coupling-constants in N-15-enriched proteins. *J. Am. Chem. Soc.* **115**, 7772–7777.
50. Güntert, P. (2004). Automated NMR structure calculation with CYANA. *Methods Mol. Biol.* **278**, 353–378.
51. Schwieters, C. D., Kuszewski, J. J. & Clore, G. M. (2006). Using Xplor-NIH for NMR molecular structure determination. *Prog. Nucl. Magn. Reson. Spectrosc.* **48**, 47–62.
52. Linge, J. P., Williams, M. A., Spronk, C. A., Bonvin, A. M. & Nilges, M. (2003). Refinement of protein structures in explicit solvent. *Proteins*, **50**, 496–506.
53. Koradi, R., Billeter, M. & Wüthrich, K. (1996). MOLMOL: a program for display and analysis of macromolecular structures. *J. Mol. Graphics*, **14**, 51–55.